tion, pp 91-93, Chester, U.K. Daresbury Laboratory, Warrington, U.K.
Jaffe, E. K., & Hanes, D. (1986) *J. Biol. Chem. 261*, 9348-9353.
Jaffe, E. K., Salowe, S. P., Chen, N. T., & De Haven, P. A. (1984) *J. Biol. Chem. 259*, 5032-5036.
Joyner, R. W., Martin, K. J., & Meehan, P. (1987) *J. Phys. C 20*, 4005-4012.
Lowry, O. H., Rosebrough, N. J., Farr, A. L., & Randall, R. J. (1951) *J. Biol. Chem. 193*, 265-275.
Matheis, L. F. (1964) *Phys. Rev. A133*, 1399.
Mauzerall, D., & Granick, S. (1956) *J. Biol. Chem. 219*, 435-446.
Morrel, C., Baines, J. T. M, Campbell, J. W., Diakun, G. P., Dobson, B. R., Greaves, G. N., & Hasnain, S. S. (1989) *Daresbury EXAFS Users' Manual*, Daresbury Laboratory, Warrington, U.K.
Pendry, J. B. (1974) *Low Energy Electron Diffraction*, Academic Press, New York.
Perutz, M. F., Hasnain, S. S., Duke, P. J., Sessler, J. L., & Hahn, J. E. (1982) *Nature 295*, 535-538.
Pilz, I., Schwarz, E., Vuga, M., & Beyersmann, D. (1990) *Biol. Chem. Hoppe-Seyler* (in press).
Schlösser, M., & Beyersmann, D. (1987) *Biol. Chem. Hoppe-Seyler 368*, 1469-1477.
Shemin, D. (1972) *Enzymes (3rd Ed.) 7*, 323-337.
Shemin, D. (1976) *Philos. Trans. R. Soc. London, B 273*, 109-115.
Sommer, R., & Beyersmann, D. (1984) *J. Inorg. Biochem. 20*, 131-145.
Strange, R. W., Blackburn, N. J., Knowles, P. F., & Hasnain, S. S. (1987) *J. Am. Chem. Soc. 109*, 7157-7162.
Tsukamoto, I., Yoshinga, T., & Sano, S. (1979) *Biochim. Biophys. Acta 570*, 167-178.
Tsukamoto, I., Yoshinga, T., & Sano, S. (1980) *Int. J. Biochem. 12*, 751-756.
Ward, W. H. J., & Fersht, A. R. (1988) *Biochemistry 27*, 1041-1049.
Wetmur, J. G., Bishop, D. F., Cantelmo, C., & Desnick, R. J. (1986) *Proc. Natl. Acad. Sci. U.S.A. 83*, 7703-7707.

Conformational Preferences of Synthetic Peptides Derived from the Immunodominant Site of the Circumsporozoite Protein of *Plasmodium falciparum* by ^{1}H NMR†

H. Jane Dyson,* Arnold C. Satterthwait,* Richard A. Lerner, and Peter E. Wright

Department of Molecular Biology, Research Institute of Scripps Clinic, 10666 North Torrey Pines Road, La Jolla, California 92037

Received January 22, 1990; Revised Manuscript Received April 12, 1990

ABSTRACT: Proton nuclear magnetic resonance and ultraviolet circular dichroism spectroscopy have been used to probe the conformational ensemble of the tandemly repeating tetrapeptide unit of the circumsporozoite coat protein of the malaria parasite *Plasmodium falciparum*. Peptides based on the Asn-Ala-Asn-Pro and Asn-Pro-Asn-Ala cadences and composed of one to three tetrapeptide units were synthesized and examined using one- and two-dimensional NMR spectroscopy. The chemical shift of the amide protons, the temperature dependence of the amide proton chemical shift, and the patterns of NOE connectivities in the various peptides give evidence for the presence of a substantial population of folded conformers in several of the peptides in water solution at pH 5.0. Correlations between the behavior of the tandemly repeated units in different peptides have been used to infer the structure(s) of the folded conformers. The data are consistent with the presence of turnlike structures stabilized by hydrogen bonding of the backbone amide protons of the alanines and the asparagine residues preceding them. Specific differences in the strengths of NOEs between peptides of different lengths indicate that the folded structure is considerably stabilized by the presence of the asparagine residue following the alanine. Differences between peptides with different cadences of the tandemly repeating unit indicate that a repeating structural motif is formed by the Asn-Pro-Asn-Ala-(Asn) cadence.

Recent advances in the molecular biology of malaria parasites and new developments in vaccine design have led to vigorous efforts to design effective malaria vaccines (Miller et al., 1986). Synthetic peptide vaccines based on cognate sequences found on the surfaces of sporozoites (Herrington et al., 1987) and merozoites (Patarroyo et al., 1988) have undergone clinical trials and show promise of protection. In order to produce effective vaccines, a strategy of rational design of the peptide immunogens is desirable. One promising approach is the design of peptide immunogens based on the known structure of components of the various forms of the parasite.

In general, peptide vaccines elicit a variety of antibodies, only some of which may bind tightly to the cognate sequence in the native protein or the pathogen. This is presumably due to the variety of conformers accessible to small, flexible peptides. If the structure of the conformer which induces protein-reactive antibodies could be determined, then it should

† This research was supported by Grant PO1 CA27498 from the National Institutes of Health and by the MacArthur Foundation.
* Address correspondence to these authors.

0006-2960/90/0429-7828$02.50/0

be possible to induce a selective response by using a conformationally restricted, perhaps covalently bonded, immunogen. Preliminary studies incorporating this idea have been published (Satterthwait et al., 1989).

In previous investigations of the solution conformation of immunogenic peptides in water solution, we have frequently observed conformational preferences for folded forms [reviewed in Dyson et al. (1988a)]. The peptides studied include sequences from influenza virus hemagglutinin (Dyson et al., 1985), *Themiste zostericola* myohemerythrin (Dyson et al., 1988b), and myoglobin (Waltho et al., 1989). In all of these peptides, a strong conformational preference for folded forms was found, using ^{1}H nuclear magnetic resonance (NMR)[1] methods, without, in many cases, any indication of structure from the circular dichroism (CD) spectrum. This is consistent with a hypothesis which suggests that the structured forms seen in solution are in rapid dynamic equilibrium with extended-chain forms and that the structures in many cases are local, and do not extend far enough to be observable by CD (Wright et al., 1988).

The immunodominant epitope of the infective form of *Plasmodium falciparum*, the sporozoite, is a tandemly repeating tetrapeptide, Asn-Ala-Asn-Pro (NANP), which comprises a region of the circumsporozoite protein covering the surface of the parasite (Nussenzweig & Nussenzweig, 1985). In this paper, we report the results of ^{1}H NMR studies on the conformations of several synthetic peptides with sequences corresponding to the tandemly repeated region. An NMR study has been published (Esposito et al., 1989) which reports no observable structure in tandemly repeating units in water solution, with traces of structure observed in methanol solution. We observe in water solution the presence of forms containing conformational preferences for local and/or helical structures, in rapid dynamic equilibrium with extended-chain forms. The implications of these observations for the design of anti-sporozoite vaccines will be discussed elsewhere.

Materials and Methods

Peptide Synthesis. Six synthetic peptide sequences corresponding to several units and cadences of the tandemly repeating unit of the *P. falciparum* circumsporozoite protein tandemly repeating unit were prepared. In each peptide, the N-terminal amino group was blocked by acetylation and the C-terminal carboxyl group by amidation. The peptide sequences were NANP, $(NANP)_2$, $(NANP)_3$, NPNA, $(NPNA)_2$, and $(NPNA)_3$. Peptides were synthesized by the Merrifield solid-phase method, on 2.5 g of benzhydrylamine resin (Chemical Dynamics, 0.7 mequiv/g, 1% cross-linked). Standard protocols were used for coupling *t*-Boc amino acids (Bachem), using a large type B reaction vessel and valving system (Stewart & Young, 1984). Coupling reactions were repeated where necessary to give >99.7% reaction, as determined by the Kaiser ninhydrin test (Kaiser et al., 1970). Peptides were acetylated on the resin with acetic anhydride/diisopropylethylamine/dimethylformamide (1:1:8) for 1 h and were cleaved from the resin with HF at 0 °C for 1 h. Purification to >98% homogeneity was achieved by using HPLC on a RP-18 Licrosorb column (EM Science, 1 × 25 cm, 7-μm particles), using a 0.1% trifluoroacetic acid and 6–40% water/acetonitrile gradient, eluting at 3 mL/min for 30 min.

Preparation of Samples for NMR Spectroscopy. Samples were prepared from lyophilized peptides by dissolving 15 mg in 0.1 M deuterioacetate buffer, pH 5.0, in 90% ^1H_2O/10% ^2H_2O, to a final volume of 0.5 mL. An internal standard of 5 μL of 0.06 M dioxane in ^2H_2O was routinely added.

Circular Dichroism Spectroscopy. Samples were 400 μM in water. Spectra were recorded on an Aviv 61DS CD spectrophotometer, using a 1-mm path cell at 5 °C. An average of 5–10 spectra were used to obtain each data set; three-point smoothing was applied to the data.

^{1}H NMR Spectroscopy. All NMR spectra were recorded on a Bruker AM500 spectrometer equipped with digital phase-shifting hardware, or on a Bruker MSL300 spectrometer. The dioxane resonance was used as an internal standard, but all spectra are referenced to TSS at 0 parts per million (ppm).

Phase-sensitive two-dimensional NMR spectra were used for sequential assignment of the proton resonances and for detection of structure. They include two-dimensional correlated (COSY) spectra (Marion & Wüthrich, 1983) or double quantum filtered COSY (Rance et al., 1983) and two-dimensional nuclear Overhauser effect (NOESY) spectra (Jeener et al., 1979) or rotating-frame NOESY (ROESY) spectra (Bothner-By et al., 1984). All assignments were obtained using solutions in 90% ^1H_2O/10% ^2H_2O. Solvent suppression was achieved in all cases using gated irradiation at the appropriate frequency. Spectra were recorded using TPPI (Drobny et al., 1979) for quadrature detection in ω_1. Mixing times in NOESY experiments were typically 600 ms, and in ROESY experiments were typically 150 ms. Under the conditions of the experiments, no spin diffusion was expected or observed. Spectral widths were typically 9 ppm in both dimensions, and 512 t_1 points were routinely acquired, with 2048 complex points for each free induction decay. The number of scans per t_1 point was usually 64 or 32.

Processing of 2D NMR data was done on a Sun3 workstation equipped with a Sky Warrior array processor, using software provided by Dr. Dennis Hare. Spectra were Fourier transformed using Lorentzian-to-Gaussian weighting or phase-shifted sine-bell window functions. The quality of the NOESY spectra was improved by the use of linear base line correction (Zuiderweg et al., 1985; Dyson et al., 1988c) and by t_1 ridge suppression (Otting et al., 1986). A small first-order phase adjustment was applied in ω_1 to correct for error introduced by resonance offset effects (Dyson et al., 1988c).

The temperature dependence of the amide proton chemical shift was calculated for each peptide by using one-dimensional spectra recorded at a minimum of seven temperatures between 274 and 310 K. Temperature calibration was performed with methanol (VanGeet, 1969). Assignments of resonances were checked by two-dimensional spectroscopy at two temperatures. The $^3J_{HN\alpha}$ coupling constant was estimated from the separation of the two components of the doublet amide proton resonance where this resonance was resolved in the one-dimensional spectrum of the peptide. For overlapped resonances, estimates of $^3J_{HN\alpha}$ were made from peak-to-peak separation in the NH–C$^\alpha$H COSY cross-peaks for each amide proton.

Results

The amide proton regions of the one-dimensional spectra of the six peptides Ac-NANP-NH_2, Ac-$(NANP)_2$-NH_2, Ac-$(NANP)_3$-NH_2, Ac-NPNA-NH_2, Ac-$(NPNA)_2$-NH_2, and Ac-$(NPNA)_3$-NH_2 are shown in Figure 1. (Hereafter, the

[1] Abbreviations: NMR, nuclear magnetic resonance; NOE, nuclear Overhauser effect; HPLC, high-performance liquid chromatography; COSY, two-dimensional correlated spectroscopy; NOESY, two-dimensional nuclear Overhauser effect spectroscopy; $d_{\alpha N}(i,j)$, $d_{NN}(i,j)$, etc., intramolecular distance between protons C$^\alpha$H and NH, NH and NH, etc. on residues i and j; ppm, parts per million; TPPI, time-proportional phase incrementation; TSS, (trimethylsilyl)propanesulfonic acid.

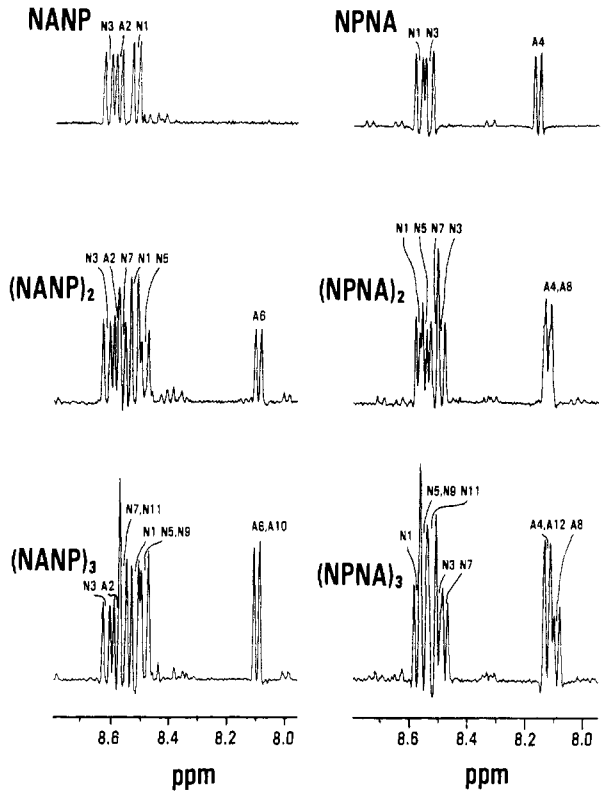

FIGURE 1: Portion of the 278 K one-dimensional spectrum of each of the peptides shown. Each peptide was dissolved in 0.1 M deuterioacetate buffer, pH 5.0, in 90% ^1H_2O/10% ^2H_2O. The region shown encompasses the resonances of the backbone amide protons. All spectra are at 300 MHz.

peptides will be referred to without explicit reference to the N- and C-terminal protecting groups.) The spectra show the presence of a small quantity of a minor component, which may be due to cis–trans isomerism about one or more of the proline residues. This component is less than 10% of the major component. The amide proton resonances of the major component for each peptide fall into two classes, a downfield set containing the majority of the signals and an upfield set. For the peptides $(NANP)_n$, there are 0, 1, and 2 resonances in the upfield set, for $n = 1$, 2, and 3, respectively. For the peptides $(NPNA)_n$, there are 1, 2, and 3 resonances in the upfield set for $n = 1$, 2, and 3. This indicates the existence of a difference in the conformational preferences of the peptides according to the cadence of the repeat unit. The amino acids with NH resonances in the upfield set have been unambiguously identified by using COSY spectra (for example, Figure 2) to be alanines. Furthermore, the differences between the two sets of peptides show that these resonances must be due to alanine in the sequence PNA.

The sequential assignment of the resonances in the spectra of the longer peptides poses problems due to the resonance overlap caused by duplication of the proton environments in the repeating units. Nevertheless, since resonances were in general sufficiently well resolved at 500 MHz, assignments were completed. The resonance assignments for the peptides are summarized in Table I.

As well as providing information essential to the sequential assignment of resonances, the NOESY spectrum also provides information on the types of conformers present in solution. This information is in the form of NOE connectivities which would not normally be observed for short peptides in extended-chain conformations. This information has been summarized (Dyson et al., 1988b,c). Briefly, when the peptide sequence is present in extended-chain forms only, NOE connectivities between the $C^\alpha H$ of a given residue i and the NH of the following residue $i + 1$ [termed $d_{\alpha N}(i,i+1)$ NOE connectivities] are strong, and $d_{NN}(i,i+1)$ NOE connectivities do not appear. If the peptide has a significant population of forms which contain turns or helices (α region of ϕ, ψ space), $d_{NN}(i,i+1)$ NOE connectivities are observed, and the $d_{\alpha N}(i,i+1)$ NOE connectivities may be weaker, depending on the relative populations of conformers in the β and α regions of ϕ,ψ space. In addition, medium-range NOE connectivites are observed when helices and turns are formed. These include $d_{\alpha N}(i,i+2)$

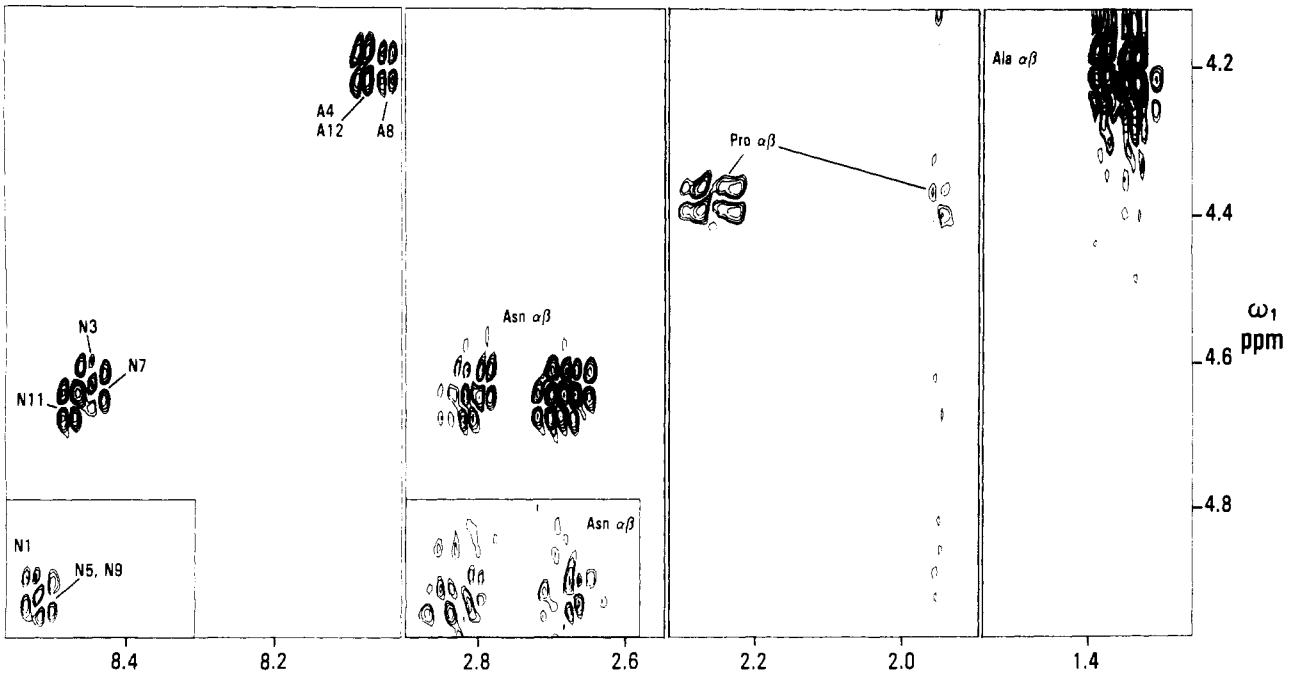

FIGURE 2: Portions of a 500-MHz 2QF COSY spectrum of $(NPNA)_3$ at 278 K. Solution conditions were as for Figure 1. The inset portions of the spectrum (containing the Asn-1, Asn-5, and Asn-9 NH–$C^\alpha H$ and $C^\alpha H$–$C^\beta H$ cross-peaks) are plotted at a lower contour level than the rest of the spectrum. Their low intensity in this spectrum reflects the overlap of the decoupled H_2O resonance with the $C^\alpha H$ resonance of these residues at this temperature. At other temperatures, these cross-peaks are of comparable intensity to others in the spectrum.

Table I: Assignments (ppm) for All Peptides[a]

peptide	residue	NH	$C^{\alpha}H$	$C^{\beta}H$	$C^{\gamma}H$	$C^{\delta}H$
(1) NANP	Asn-1	8.51	4.65	2.68, 2.80		
	Ala-2	8.57	4.29	1.36		
	Asn-3	8.61	4.96	2.67, 2.84		
	Pro-4		4.37	2.26, 1.99	2.01	3.75
(2) $(NANP)_2$	Asn-1	8.52	4.65	2.68, 2.80		
	Ala-2	8.58	4.27	1.35		
	Asn-3	8.61	4.95	2.72, 2.88		
	Pro-4		4.40	2.29, 1.98	2.00	3.80
	Asn-5	8.48	4.67	2.71, 2.85		
	Ala-6	8.09	4.24	1.38		
	Asn-7	8.56	4.96	2.70, 2.85		
	Pro-8		4.38	2.26, 1.98	2.01	3.74
(3) $(NANP)_3$	Asn-1	8.51	4.64	2.7, 2.8		
	Ala-2	8.57	4.26	1.35		
	Asn-3	8.61	4.91	2.72*, 2.86*		
	Pro-4		4.40	2.28*, 1.96*	2.0*	3.79*
	Asn-5	8.48	4.66	2.71*, 2.84*		
	Ala-6	8.09	4.22	1.37*		
	Asn-7	8.55	4.92	2.72*, 2.86*		
	Pro-8		4.40	2.28*, 1.96*	2.0*	3.79*
	Asn-9	8.48	4.66	2.71*, 2.84*		
	Ala-10	8.09	4.22	1.37*		
	Asn-11	8.55	4.92	2.72*, 2.86*		
	Pro-12		4.36	2.28*, 1.96*	2.0*	3.79*
(4) NPNA	Asn-1	8.57	4.95	2.69, 2.87		
	Pro-2		4.43	2.30, 1.95	2.0	3.79, 3.86
	Asn-3	8.53	4.69	2.74, 2.87		
	Ala-4	8.16	4.23	1.41		
(5) $(NPNA)_2$	Asn-1	8.57	4.95	2.70, 2.85		
	Pro-2		4.41	2.27, 1.95	2.0*	3.78*, 3.82*
	Asn-3	8.49	4.66	2.71, 2.85		
	Ala-4	8.13	4.24	1.37		
	Asn-5	8.55	4.97	2.70, 2.84		
	Pro-6		4.42	2.29, 1.93	2.0*	3.78*, 3.82*
	Asn-7	8.52	4.69	2.73, 2.87		
	Ala-8	8.12	4.23	1.41		
(6) $(NPNA)_3$	Asn-1	8.57	4.92	2.70, 2.83		
	Pro-2		4.39*	2.26*, 1.97*	2.0*	3.8*
	Asn-3	8.49	4.62	2.69, 2.81		
	Ala-4	8.12*	4.19*	1.38		
	Asn-5	8.54*	4.93*	2.68*, 2.85*		
	Pro-6		4.39*	2.26*, 1.97*	2.0*	3.8*
	Asn-7	8.47	4.64	2.69, 2.81		
	Ala-8	8.09	4.20	1.34*		
	Asn-9	8.54*	4.93*	2.68*, 2.85*		
	Pro-10		4.39*	2.26*, 1.97*	2.0*	3.8*
	Asn-11	8.52	4.66	2.70, 2.83		
	Ala-12	8.12*	4.20*	1.34*		

[a] Asterisks indicate COSY cross-peaks that are exactly overlapped.

Table II: Amide Proton Temperature Coefficients and $^3J_{HN\alpha}$ Coupling Constants for All Peptides[a]

peptide	residue	$-\Delta\delta/\Delta T \times 10^3$ (ppm/K)	$^3J_{HN\alpha}$ (Hz)
(1) NANP	Asn-1	7.04	6.9[b]
	Ala-2	7.85	6.0[b]
	Asn-3	7.64	7.1[b]
(2) $(NANP)_2$	Asn-1	7.02	6.9[c]
	Ala-2	8.00	6.0[c]
	Asn-3	7.77	7.1[b]
	Asn-5	5.96	7.5[b]
	Ala-6	5.66	5.8[b]
	Asn-7	8.09	7.4[c]
(3) $(NANP)_3$	Asn-1	7.01	7.5[c]
	Ala-2	7.96	6.0[c]
	Asn-3	7.72	7.1[b]
	Asn-5	6.02	7.5*[c]
	Ala-6	5.74	5.9*[b]
	Asn-7	8.03	7.5*[c]
	Asn-9	6.02	7.5*[c]
	Ala-10	5.74	5.9*[b]
	Asn-11	8.03	7.5*[c]
(4) NPNA	Asn-1	7.97	6.9[b]
	Asn-3	6.21	7.5[b]
	Ala-4	6.12	6.0[b]
(5) $(NPNA)_2$	Asn-1	7.95	6.8[b]
	Asn-3	6.13	7.5[c]
	Ala-4	6.03	5.9*[b]
	Asn-5	7.88	7.2[b]
	Asn-7	6.11	7.5[c]
	Ala-8	5.93	5.9*[b]
(6) $(NPNA)_3$	Asn-1	8.12	7.0[c]
	Asn-3	6.11	7.5[c]
	Ala-4	6.04	5.9*[b]
	Asn-5	7.93	7.5*[c]
	Asn-7	5.96	7.5[c]
	Ala-8	5.67	5.9[b]
	Asn-9	7.93	7.5*[c]
	Asn-11	6.09	7.5[c]
	Ala-12	5.93	5.9*[b]

[a] Asterisks are values estimated for two exactly overlapped NH–$C^{\alpha}H$ COSY cross-peaks. [b] Source for $^3J_{HN\alpha}$: one-dimensional spectrum at 278 K. [c] Source for $^3J_{HN\alpha}$: COSY spectrum at 278 K.

NOE connectivities [for turns (Dyson et al., 1988c) and nascent helix (Dyson et al., 1988b)] and $d_{\alpha N}(i,i+3)$ and $d_{\alpha\beta}(i,i+3)$ NOE connectivities [for helices (Dyson et al., 1988b; Wüthrich et al., 1984)].

Portions of the NOESY spectrum of the peptides $(NPNA)_3$ and $(NANP)_3$ are shown in Figures 3 and 4. For both peptides, there are strong $d_{\alpha N}(i,i+1)$ NOE connectivities throughout the peptide, including connectivities to the proline $C^{\delta}H$ protons, which may be used in place of the NH for proline (Wüthrich et al., 1984). This indicates that extended-chain forms are present in the conformational ensemble of these peptides. In addition, both peptides show strong $d_{NN}(i,i+1)$ NOE connectivities, indicating the presence of significant populations of backbone conformations in the α region of ϕ,ψ space. The NOE connectivities between the proline $C^{\delta}H$ protons and the NH's of adjacent residues are by comparison much weaker than the $d_{NN}(i,i+1)$ connectivities seen in other parts of the peptide. Figures 3 and 4 also show the presence of $d_{\alpha N}(i,i+2)$ NOE connectivities.

The NOE connectivities observed for the peptides are summarized in Figure 5. It should be noted that some of the NOE connectivities may well be present but are obscured by resonance overlap, by proximity of the $C^{\alpha}H$ resonance to that of the H_2O or by proximity of cross-peaks to the spectrum diagonal. Also, the size of these peptides is not ideal for the observation of NOE connectivities in NOESY spectra (Ernst et al., 1987). The ROESY spectrum was particularly useful for the smaller peptides, where the NOESY spectrum gives very little information. A ROESY spectrum acquired for $(NANP)_3$ gave information identical with the NOESY spectrum of this peptide. The ROESY spectrum of NPNA (Figure 6) shows the presence of similar NOE connectivities in the shorter peptide as in the longer ones.

Other NMR data can be used to give information on the conformational preferences of peptides. These include the temperature coefficient of the amide proton chemical shift and the $^3J_{HN\alpha}$ coupling constant (Dyson et al., 1988c). These data are shown for each peptide in Table II. Coupling constant data can be gained directly from the one-dimensional spectrum for the shorter peptides, and from COSY spectra for the longer peptides. In some cases, the NH–$C^{\alpha}H$ COSY cross-peaks of two different residues are exactly overlapped at all accessible temperatures, which precludes measurement of accurate

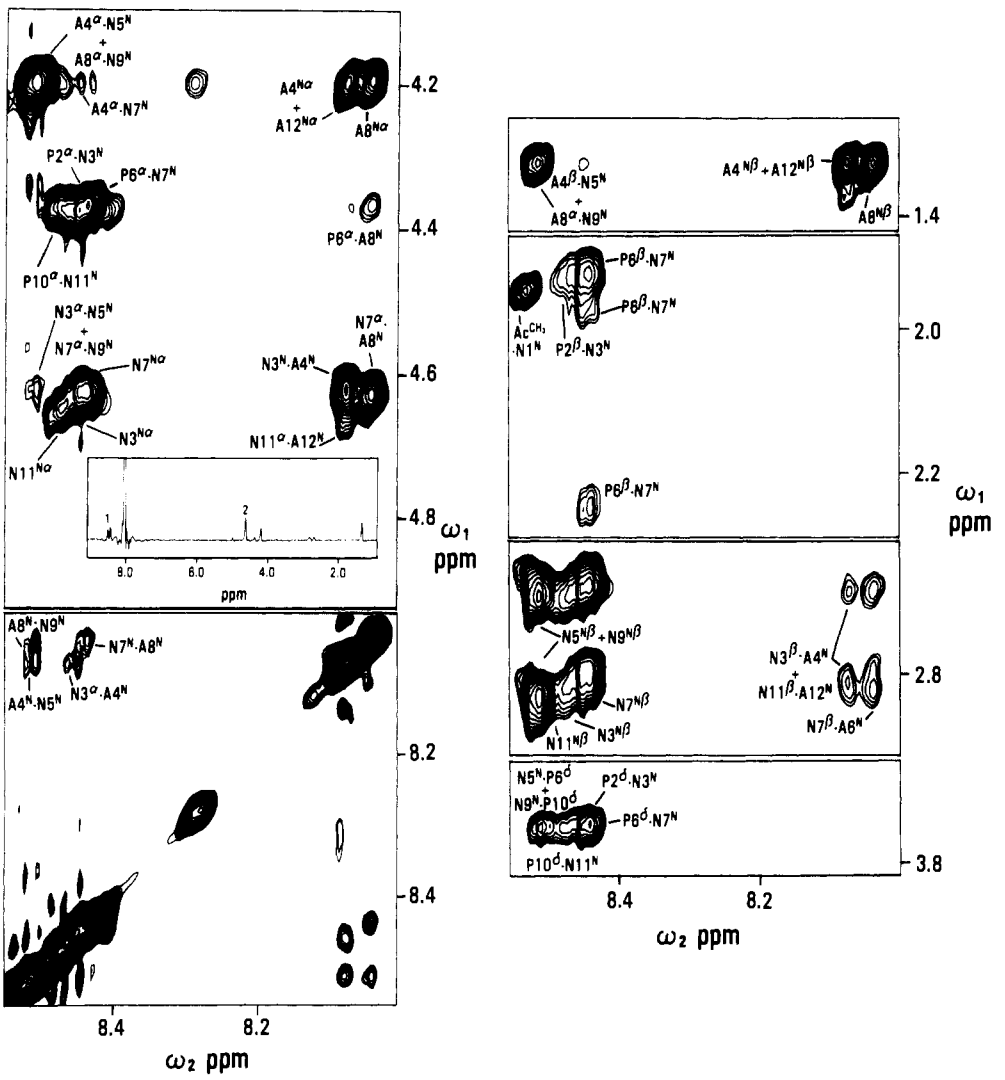

FIGURE 3: Portions of a 500-MHz NOESY spectrum of $(NPNA)_3$ at 278 K. Solution conditions were as for Figure 1. The mixing time (τ) was 600 ms. The regions showing cross-peaks to the amide protons are shown. Inset: Cross section through the spectrum at a column corresponding to the chemical shift of Ala-8, provided to demonstrate the relative magnitudes of the $d_{NN}(i,i+1)$ NOESY cross-peaks (labeled 1) and the $d_{\alpha N}(i,i+1)$ cross-peaks (labeled 2).

coupling constant data. Values obtained from the one- and two-dimensional spectra of the peptides are shown in Table II, together with an indication of uncertainty due to overlap where it occurs.

In principle, the CD spectrum can give information on the conformation of polypeptide chains in solution (Adler et al., 1973; Woody, 1974; Brahms & Brahms, 1980). The CD spectra of $(NPNA)_3$ and $(NANP)_3$ are shown in Figure 7.

Discussion

Evaluation of NOE Results. The NOE spectra of the six peptides studied in this work show evidence of the presence of structured forms other than the extended-chain (β) conformations to be expected for linear peptides in water solution (Brant et al., 1967). The $d_{NN}(i,i+1)$ NOE connectivities seen in the NOESY spectra of $(NANP)_3$ and $(NPNA)_3$ (Figures 3 and 4) and in the ROESY spectra of $(NANP)_2$ and $(NPNA)_2$ (data not shown) are of comparable intensity to the $d_{\alpha N}(i,i+1)$ NOEs to the same amide proton. This is demonstrated in the inset to Figure 3, which shows a single column of the two-dimensional spectrum plotted in Figure 3. By contrast, the ROESY spectrum of NPNA (Figure 6) shows only a very weak $d_{NN}(i,i+1)$ NOE between Asn-3 and Ala-4. A weak NOE is also present between the C-terminal amide blocking group and the NH of Ala-4, as well as a much stronger connectivity between the blocking group and the Ala-4 $C^{\alpha}H$ (data not shown). The NOE experiments do not specifically exclude the presence of $d_{NN}(i,i+1)$ NOE connectivities in the peptide NANP and in the N-terminal NANP units of $(NANP)_2$ and $(NANP)_3$, since the NOEs would be unobservable due to proximity of the cross-peaks to the diagonal. However, other NMR data indicate that this unit is indeed significantly different from the NPNA units. For each of the 8- and 12-residue peptides, the strong $d_{NN}(i,i+1)$ NOE connectivities are present between the alanine NH and the asparagine NH's preceding and following it in the peptide sequence. This means that a significant population in the conformational ensemble of the peptide in solution has a backbone conformation in the α region of ϕ,ψ space at these positions (Wright et al., 1988). The relative size of these NOEs compared with the $d_{NN}(i,i+1)$ NOEs for the same residue indicates that the α conformations are quite well populated.[2] Whether the $d_{NN}(i,i+1)$ NOEs observed for a given peptide arise from the same or different conformers is not obvious, and both possibilities will be considered in the

[2] We emphasize that we use the term α conformation to signify states in which *local* backbone dihedral angles are in the α region of ϕ,ψ space; these are not necessarily helical states, in which several *successive* residues would have ϕ,ψ angles in the α region.

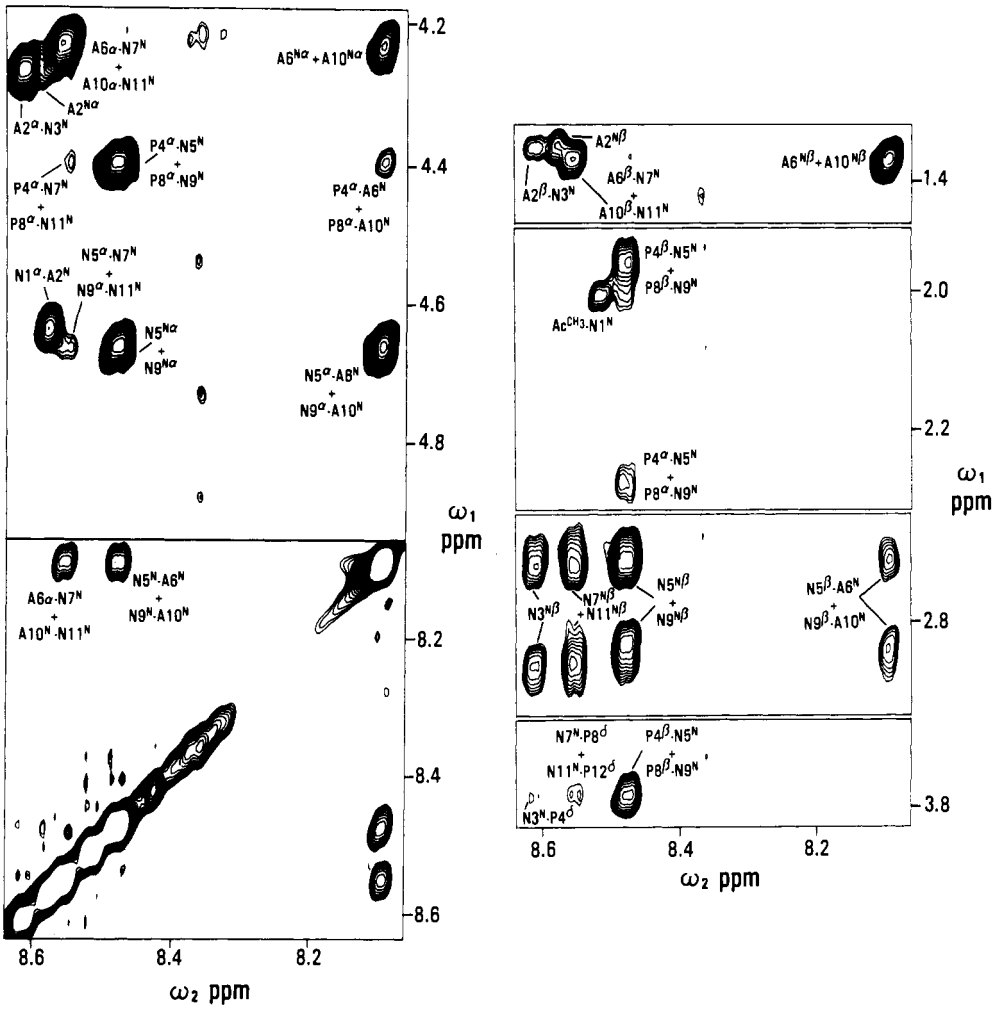

FIGURE 4: Portions of a 500-MHz NOESY spectrum of $(NANP)_3$ at 278 K. Solution conditions were as for Figure 1. The mixing time τ was 600 ms.

structural discussions to follow. Medium-range $d_{\alpha N}(i,i+2)$ NOE connectivities are also present in all instances where a NPNAN unit is present. C-Terminal NPNA units are apparently less structured. This suggests that the conformers for which the backbone conformation is α participate in turnlike structures. Minor $d_{\alpha N}(i,i+3)$ NOE connectivities may be present in some NOESY spectra of the longer peptides, which give a further indication as to the likely structure of the folded conformers. Other NMR parameters, such as temperature coefficients, chemical shifts, and coupling constants, can also give information on conformational preferences.

Temperature Coefficients and Coupling Constants. The differences seen in the temperature coefficients between the amide protons in different cadences of the sequence are very consistent, and will be discussed below. The actual values of the temperature coefficients, for example, for the Ala NH of the NPNA unit, would not normally be taken to reflect extensive hydrogen bonding: values below 6×10^{-3} ppm K^{-1} would usually be expected in this case [see Dyson et al. (1988c) and references cited therein]. Three factors can be considered here. First, the consistency of the values between peptides indicates some common structural motif is present. Second, the NOE evidence indicates an extensive population of β conformers, which would dilute the effects of hydrogen bonding on the temperature coefficients, since they are population-weighted averages. Third, turn and helix conformations are quite often present in high populations without any significant intrachain hydrogen bonding (Rose et al., 1985; Dyson et al., 1988c). Given these considerations, together with the strong indications of folded structure obtained from the NOE experiments, we have proceeded to use the temperature coefficient data as an indication of types of conformers, without placing great emphasis on the absolute magnitude of the coefficients.

By contrast, the $^3J_{HN\alpha}$ coupling constants (Table II) do not show such significant differences between residues in different peptides. The residues with low temperature coefficients do appear to have somewhat lower $^3J_{HN\alpha}$ coupling constants. As has been noted elsewhere (Dyson et al., 1988c), the coupling constant is one of the least sensitive parameters to the population of conformers in the α region of ϕ,ψ space.

The temperature coefficient data (Table II), taken together with the differences in chemical shift of the amide protons in the peptides (Table I), indicate a significantly different environment for the amide protons of residues in peptides with different portions of the tandemly repeating unit present. In particular, within the NPNA unit, present in five of the six peptides, the chemical shift of the alanine NH is shifted upfield, and its temperature coefficient is lower by about 2×10^{-3} ppm K^{-1} than, for example, the alanine NH from the peptide NANP. Furthermore, the Ala-2 NH in NANP, $(NANP)_2$, and $(NANP)_3$ behaves differently from all of the other Ala NH's, and its behavior is almost identical in these three peptides. Thus, the temperature coefficient of Ala-2 is about 7.9 for all three peptides, whereas those of Ala-6 in $(NANP)_2$ and $(NANP)_3$ and Ala-10 in $(NANP)_3$ are about 5.7. The values for the peptides with the NPNA cadence are consistent with this: the temperature coefficients of all alanine

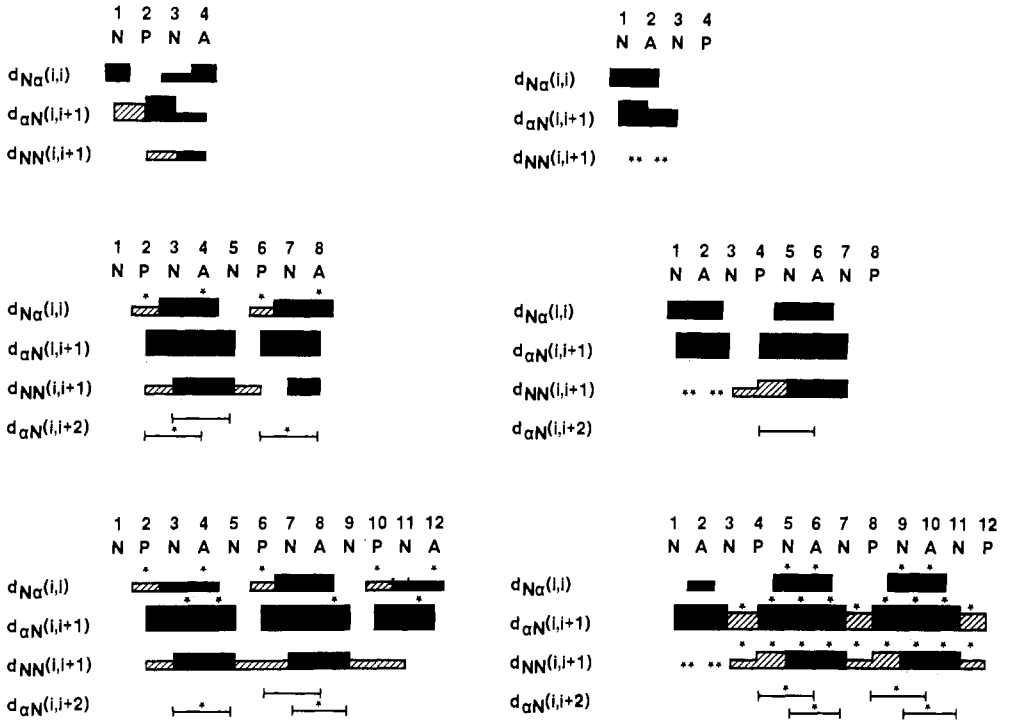

FIGURE 5: Summary of NOE connectivities observed for all peptides at 278 K. Data for NANP, NPNA, $(NANP)_2$, and $(NPNA)_2$ were obtained from 300-MHz ROESY spectra at a mixing time (spin-lock period) of 150 ms. Data for $(NANP)_3$ and $(NPNA)_3$ were obtained from the 500-MHz NOESY spectra shown in Figures 3 and 4. A single asterisk indicates NOE cross-peaks which are completely overlapped, and therefore cannot be reliably quantitated. Two asterisks indicate that the chemical shifts of the amide protons concerned are close together, so that NOE connectivities cannot be observed due to the proximity of the spectrum diagonal. Hatched boxes indicate that the connectivities are observed to the proline $C^{\delta}H$ protons (in place of the NH).

NH's are about 6.0. The Asn NH resonances fall into two distinct classes in the NPNA cadence. The Asn NH's which are located directly after a proline residue [Asn-5 in $(NANP)_2$ and $(NANP)_3$, Asn-9 in $(NANP)_3$, Asn-3 in NPNA, $(NPNA)_2$, and $(NPNA)_3$, Asn-7 in $(NPNA)_2$ and $(NPNA)_3$, and Asn-11 in $(NPNA)_3$] all have lowered temperature coefficients, similar to those of the alanine NH's. Once again, the cadence must be NPNA for this to be observed; the temperature coefficient of Asn-1 in the peptides with the cadence NANP remains high. On the other hand, the Asn NH protons which are located directly after alanine residues and/or directly before proline residues have uniformly high temperature coefficients. Apparently the cadence of the units is immaterial in this case. As for the Ala residues, the chemical shifts of the amide and $C^{\alpha}H$ protons of the Asn residues also fall into groups consistent with the groupings of temperature coefficients.

Structural Implications of the NMR and CD Data. The sequence of the tandemly repeated unit contains several elements which should bias its conformation toward helical or turn conformations. First, the sequence NPNA has a high empirical propensity for β-turn formation (Chou & Fasman, 1977, 1978). The turn prediction for this sequence is 5.4×10^{-4}, which is considerably higher than the usually quoted threshold of 0.75×10^{-4}. By contrast, the value for the sequence YPGD, which has been shown (Dyson et al., 1988c) to be present in high population as a reverse turn in water solution, is 3.8×10^{-4}. Second, the sequence NP predisposes toward helix initiation, since side-chain hydrogen-bonded asparagine residues are often found with prolines at the N-terminal of helices in proteins, and may contribute to the stability of the helix (Richardson & Richardson, 1988; Presta & Rose, 1988). The data presented herein for the synthetic peptides corresponding to different lengths and cadences of the tandemly repeating unit demonstrate that the peptide sequence has a major conformational preference for structures with an α backbone conformation at the Asn-3-Ala-4 positions of the NPNA unit. The NOE evidence strongly suggests that the structured conformers contain helical and/or reverse turns. The NMR data cannot distinguish whether these turns are present in the same conformer or are merely present as single turns in different positions as a population-weighted average. However, if the peptide is helical, rather than nascent helix [i.e., a population-weighted average of single turns (Dyson et al., 1988b)], then the CD spectrum should show evidence of helix in the form of negative ellipiticity at 222 nm (Adler et al., 1973). The ellipticity minimum at 198 nm and the lack of a significant minimum at ~220 nm are consistent with a structural model for the peptide in which there are only small populations of molecules with more than one consecutive helical turn. This is to be expected since every fourth residue is proline, which distorts helices (Piela et al., 1987). Thus, the NOE and CD evidence points toward the presence of conformers containing helical turns in the sequence NPNA, in rapid dynamic equilibrium with unfolded forms.

A lowered temperature coefficient for an amide proton is generally taken to imply some degree of protection from solvent [see Rose et al. (1985) and references cited therein]. The extent to which the coefficient is lowered, compared with the solvent-exposed value of about 8×10^{-3} ppm K^{-1}, has been used as a semiquantitative measure of the population of folded forms of the peptide (Dyson et al., 1988c). In addition, the chemical shift of the amide proton has been correlated with solvent exposure: the resonances of amide protons involved in intramolecular hydrogen bonding are shifted upfield compared to those of amides completely exposed to the stronger intermolecular hydrogen bonding from the solvent water [see Rose et al. (1985) and references cited therein]. The chemical shifts and temperature coefficients of the alanine amide protons are thus consistent with a significant population of intramo-

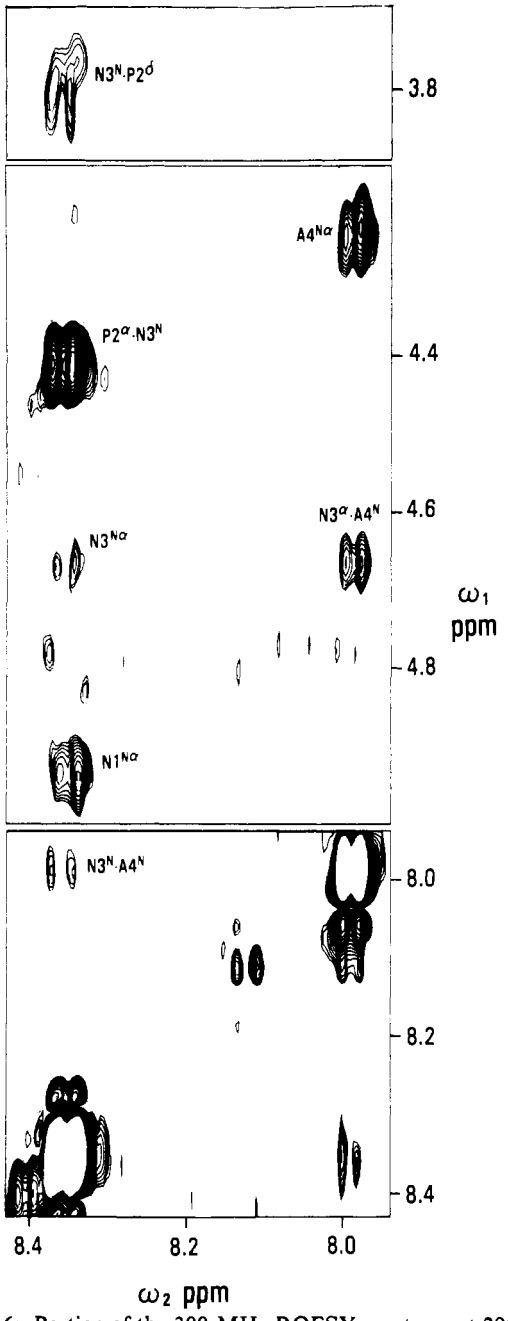

FIGURE 6: Portion of the 300-MHz ROESY spectrum at 298 K of NPNA. Solution conditions were as for Figure 1.

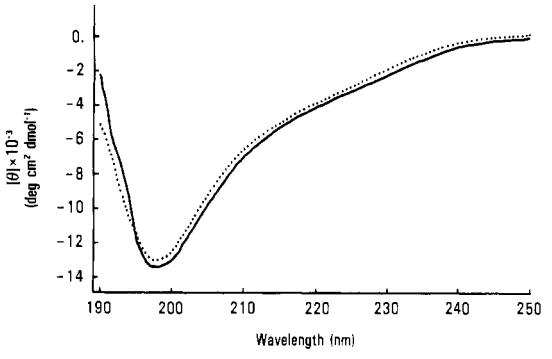

FIGURE 7: Circular dichroism spectra of $(NANP)_3$ and $(NPNA)_3$. The solutions were 400 μM in water at 5 °C.

lecularly hydrogen-bonded forms. The position of the hydrogen bond acceptor in this case can be inferred from the absence of hydrogen-bonded behavior in the N-terminal NANP unit. The acceptor in peptides containing the NPNA

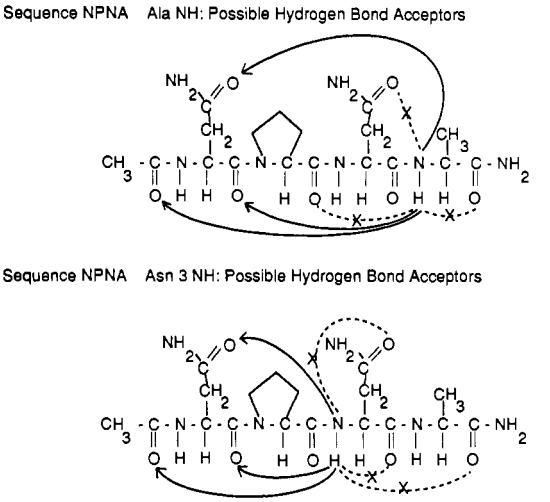

FIGURE 8: Schematic representation of the carbonyl groups capable of hydrogen bonding with the Ala-4 and Asn-3 NH's in NPNA. Solid lines indicate allowed connections; dashed lines indicate those connections eliminated by consideration of the differing behavior of the amide protons in the peptide NANP.

sequence must thus be present in the N-terminal NP sequence. Possible candidates include the backbone carbonyl group of the Asn residue preceding the Pro, the CO of the side chain of this residue, and the CO of the N-terminal acetyl group (or of the preceding Ala residue in longer peptides). The carbonyl group of the Pro and the side chain CO of the Asn preceding the Ala are eliminated, since they are present in the peptide NANP which does not exhibit this behavior (the Pro CO is replaced in this peptide by the CO of the acetyl protecting group). These possibilities are shown in Figure 8. A hydrogen bond between the Ala-4 NH and the Asn-1 backbone CO in NPNA would form a typical β-turn. The NOE connectivities observed for the NPNA unit are consistent with a tightly bent structure such as a turn conformation: $d_{\alpha N}(i,i+2)$ and strong $d_{NN}(i,i+1)$ NOE connectivities are present (Figures 3, 4, and 6). The presence of $d_{\delta N}(i,i+1)$ NOEs between the proline and the Asn which follows it can be taken as an indication that the turn conformations are, at least in some cases, of type I. Type II turns are not eliminated, however. The diagnostic NOE which distinguishes type II is a $d_{\alpha N}(2,3)$ NOE (Wüthrich et al., 1984; Dyson et al., 1988c), which exactly corresponds to the $d_{\alpha N}(i,i+1)$ NOE in the unfolded conformers. Contributions from a type II turn conformation may well be present in the observed NOE crosspeak.

The temperature coefficients of the Asn residues following Ala are uniformly high, implying that these amide protons are solvent-exposed, while those of the Asn residues preceding the Ala are uniformly low [with the consistent exception of Asn-1 in the $(NANP)_n$ peptides], implying that these protons are protected from solvent, although the upfield shift seen for the Ala amides is not observed for the Asn amides. By analogy with the Ala case above, we can argue that possible hydrogen bond acceptors for these protons can also only come from the NP sequence plus the carbonyl of the N-terminal acetyl protecting group (or the CO of the preceding Ala, where the sequence in question occurs in the middle of the peptide). These connections are summarized in Figure 8. Topological considerations make it unlikely that the CO of the Asn preceding the Pro could hydrogen bond to the NH of the Asn following the Pro (separated by four backbone bonds). (The connection between the Ala NH and the Pro CO is similarly not sterically favored, and can in any case be eliminated as described above.)

In addition to the possible singly hydrogen-bonded conformers which could be formed with either the Asn-3 or the Ala-4 NH, two possible conformer structures with both Asn-3 and Ala-4 hydrogen bonded can be derived for the NPNA unit by using these considerations. Following the numbering scheme of Figure 8, we can postulate hydrogen bonding of Asn-1 CO with Ala-4 NH, and concomitant hydrogen bonding of the CO of the acetyl protecting group with the Asn-3 NH. This satisfies both the requirement for α backbone conformation (indicated by the NOE connectivities) and the differing degrees of solvent protection of the two NH's involved (indicated by the temperature coefficients). The turn type in this case would be type I (or III, also present in 3_{10} helix). An alternative interpretation is that the side-chain carbonyl group of Asn-1 is the hydrogen bond acceptor for the NH of Asn-3. This conformer is consistent with studies (Richardson & Richardson, 1988; Presta & Rose, 1988) which implicate side-chain–backbone hydrogen bonding, especially in the sequence Asn-Pro-X, in the N-termini of helices in proteins. Specifically, it is common to observe a hydrogen bond between the side chain CO of the Asn and the peptide NH of residue $n + 2$, i.e., of residue X, which corresponds in the NPNA sequence with Asn-3. The turn type in this case would also probably be type I. Model building confirms that the two hydrogen-bonded conformers [Asn-1 CO–Ala-4 NH with (acetyl or previous residue) CO–Asn-3 NH and Asn-1 CO–Ala-4 NH with Asn-1 side-chain CO–Asn-3 NH) are both sterically allowed. From these data, it is not clear which of the two is favored in the conformer population, and it is likely that both structures are populated, though perhaps not to equal extents. For example, for stable 3_{10} helix, $d_{\alpha N}(i,i+3)$ NOEs should be visible, and these are not in general seen in the peptide NOESY spectra. Further information on the exact nature of the structures could be gained from studies of peptides with unblocked amino termini.

The isolated β-turn conformation predicted by the Chou and Fasman statistics (Chou & Fasman, 1977, 1978) for the NPNA sequence is not apparently the entire story. As well as a strong $d_{NN}(i,i+1)$ NOE connectivity between the Ala NH and that of the Asn which precedes it (as expected for a β-turn), there is a connectivity of similar strength between the Ala NH and that of the Asn which follows it (in the 8- and 12-residue peptides; see Figure 5). As well, the connectivities characteristic of the folded conformation are considerably weaker in the peptide NPNA than those in the 8- and 12-residue peptides. This may be due in part to the shortness of the peptide, where "end-fraying" effects will be more pronounced. An additional factor could well be that the folded conformation is stabilized by the presence of residues C-terminal to it. The C-termini of $(NANP)_2$ and $(NANP)_3$ show greater evidence of structure than the C-termini of $(NPNA)_2$ and $(NPNA)_3$: The d_{NN} (Asn-9-Ala-10) NOE in $(NANP)_3$ is stronger than the analogous d_{NN} (Asn-11-Ala-12) NOE in $(NPNA)_3$, for example. The nature of this stabilization and/or folding must take into account the solvent accessibility of the Asn NH following the Ala, as well as the proximity of this proton to the Ala NH [the $d_{NN}(i,i+1)$ NOE], to the $C^{\alpha}H$ of the Asn preceding the Ala [the $d_{\alpha N}(i,i+2)$ NOE], and to the $C^{\alpha}H$ of the Asn preceding the Ala [the $d_{\alpha N}(i,i+2)$ NOE; see Figure 5]. Clearly, the NH of the Asn following the Ala is not hydrogen bonded, eliminating the possibility of a continuous stretch of helix. Both nonspecific and specific interactions could be invoked to account for these observations. First, "end-fraying" could be an important factor, as mentioned previously. Second, the C-terminal Asn-Pro-NH_2 sequence could act nonspecifically, creating rotational barriers which favor non-hydrogen-bonded turns. Third, hydrogen-bonding interactions of the side-chain amides of the Asn residues following the Ala residues [Asn-11 in $(NANP)_3$, for example] with the carbonyls of preceding residues [Asn-7 or Pro-8 in $(NANP)_3$, for example] could stabilize a turnlike structure consistent with the data. If this is the case, the Asn-5 NH, while not specifically hydrogen bonded, is placed in close proximity to the carbonyls of Pro-2 and Asn-1. The behavior of the Asn-5 NH (high temperature coefficient, NOE's to Ala-4 NH and Asn-3 $C^{\alpha}H$) is very similar to Val-5 in the hemagglutinin peptides (Dyson et al., 1988c). In simulations (Wright et al., 1989), this NH participated in a bifurcated hydrogen bond together with the Asp-4 NH, to the CO at residue 1, suggesting an analogous model for the repeating unit NPNAN. Thus, the structure proposed is not a continuous helix, but rather an interlinked series of turn conformations, stabilized by, among other interactions, the presence of the side chains of the Asn residues.

The CD measurements are consistent with this: it is known that a minimum length of 7–10 residues of ordered helix is required for the observation of the strong negative ellipticity at 222 nm, characteristic of helix (Goodman, 1990). The presence of conformational fluctuations can seriously weaken the CD signal, to the point where peptides have been characterized as unstructured by CD while in fact containing quite high populations of helical conformers revealed in NMR experiments (Waltho et al., 1989). In the present case, the CD spectra do show some negative ellipticity at 222 nm, although the spectra (Figure 7) are not typical of α-helix (Adler et al., 1973). It is also not clear that the CD spectrum of the 3_{10} helix or of the N-terminal initiation region of a helix should be the same as that for the α-helix.

Several predictions of the structure of the repeating tetrapeptide unit have been made, using buildup procedure (energy minimization) calculations (Gibson & Scheraga, 1986) and molecular dynamics calculations (Brooks et al., 1987), as well as an NMR study in methanol/water mixtures (Esposito et al., 1989). Gibson and Scheraga (1986) found two structures of minimum energy, both helical in nature, but neither exhibiting the specific conformational features observed in our experiments, that is, in neither structure would there be the close approach of sequential amide protons and $C^{\alpha}H(i)$–NH-$(i+2)$ protons shown by the NMR data (Figure 5). The two conformations both show hydrogen bonding between the asparagine side chains, a possibility not incompatible with our NMR data. However, our NOE spectra do not show the interactions between the side chains of Pro and Ala predicted in these structures. No discussion of backbone hydrogen bonding was made by Gibson and Scheraga, but the figures in their paper do not show any hydrogen-bonding interactions which could be consistent with our NMR data for the Asn and Ala amide protons. Brooks et al. (1987) postulate an extended helical ribbon, termed a 12_{38} helix, with interhelical hydrogen bonding stabilizing an oligomeric structure. We have found no evidence of peptide oligomerization or aggregation in the experiments reported herein; for example, no concentration dependence of the chemical shift or line width was seen in the NMR experiments, and the CD spectra were concentration independent. In the Brooks et al. model, there is also apparently no consistency with our experimental data. This may be due to the intrachain packing of their lowest energy conformation, which would not be detected in the short peptides employed in this study. On the basis of proton NMR experiments conducted in methanol/water mixtures, Esposito

et al. (1989) postulate a structure for the peptide $(NANP)_2NA$, closely related to the peptides we have studied. The analysis of the NMR data by Esposito et al. is flawed in that they try to rationalize all of the NMR data on the basis of a single structure. Since these molecules are unconstrained linear peptides in hydrogen-bonding solvents, they are most likely to exist as a rapidly exchanging mixture of conformers. Our own NMR and CD experiments [reviewed in Wright et al. (1988)] offer no information to contradict this well-established dogma. The structure suggested by these authors also cannot be reconciled with our NMR data, perhaps due to the difference in solvent conditions.

In conclusion, our NMR and CD studies of the tandemly repeating peptide sequence from *P. falciparum* have shown that even in quite short peptides in water solution the sequence NPNA contains a significant population of hydrogen-bonded, folded conformers. The data are consistent with several possible conformations, all tightly bent at the proline residue, but with differing backbone hydrogen-bonding patterns. The peptides consistently exhibit a cadence which identifies the structural unit as Asn-Pro-Asn-Ala-Asn, rather than the more commonly quoted Asn-Ala-Asn-Pro.

The observation of folded conformers provides a rationale for the effectiveness of these peptides as immunogens and potential synthetic vaccines. Antibodies with binding pockets which mirror the surface of these conformers would be more likely to bind to the surface of a native protein which retained these shapes. To the extent that this is so, the effectiveness of these peptides as vaccines could be enhanced by further restricting their conformation to the one or more structures which may be formed in water. The suggested local conformations consistent with the NOE and other NMR data provide structures which are testable in NMR and immunological experiments using chemicaally modified peptides. Initial studies (Satterthwait et al., 1989) indicate that this approach will be of interest since antibodies to a chemically modified, conformationally restricted NPNA repeat cross-react with living sporozoites.

ACKNOWLEDGMENTS

We are grateful to Beth Larson for assistance with preparation of the manuscript.

REFERENCES

Adler, A. J., Greenfield, N. J., & Fasman, G. D. (1973) *Methods Enzymol. 27*, 675–735.

Bothner-By, A. A., Stephens, R. L., Lee, J., Warren, C. D., & Jeanloz, R. W. (1984) *J. Am. Chem. Soc. 106*, 811–813.

Brahms, S., & Brahms, J (1980) *J. Mol. Biol. 138*, 149–178.

Brant, D. A., Miller, W. G., & Flory, P. J. (1967) *J. Mol. Biol. 23*, 47–65.

Brooks, B. R., Pastor, R. W., & Carson, F. W. (1987) *Proc. Natl. Acad. Sci. U.S.A. 84*, 4470–4474.

Chou, P. Y., & Fasman, G. D. (1977) *J. Mol. Biol. 115*, 135–175.

Chou, P. Y., & Fasman, G. D. (1978) *Adv. Enzymol. Relat. Areas Mol. Biol. 47*, 45–148.

Drobny, G., Pines, A., Sinton, S., Weitekamp, D., & Wemmer, D. (1979) *Symp. Faraday Soc. 13*, 49–55.

Dyson, H. J., Cross, K. J., Houghten, R. A., Wilson, I. A., Wright, P. E., & Lerner, R. A. (1985) *Nature (London) 318*, 480–483.

Dyson, H. J., Lerner, R. A., & Wright, P. E. (1988a) *Annu. Rev. Biophys. Biophys. Chem. 17*, 305–324.

Dyson, H. J., Rance, M., Houghten, R. A., Wright, P. E., & Lerner, R. A. (1988b) *J. Mol. Biol. 201*, 201–217.

Dyson, H. J., Rance, M., Houghten, R. A., Lerner, R. A., & Wright, P. E. (1988c) *J. Mol. Biol. 201*, 161–200.

Ernst, R. R., Bodenhausen, G., & Wokaun, A. (1987) *Principles of Magnetic Resonance in One and Two Dimensions*, Clarendon Press, Oxford.

Esposito, G., Pessi, A., & Verdini, A. S. (1989) *Biopolymers 28*, 225–246.

Gibson, K. D., & Scheraga, H. A. (1986) *Proc. Natl. Acad. Sci. U.S.A. 83*, 5649–5653.

Goodman, M. (1990) *Proc. Am. Pept. Symp., 11th*, 3–29.

Herrington, D. A., Clyde, D. F., Losonsky, G., Cortesia, M., Murphy, J. R., Davis, J., Baqar, S., Felix, A. M., Heimer, E. P., Gillessen, D., Nardin, E., Nussenzweig, R. S., Nussenzweig, V., Hollingdale, M. R., & Levine, M. M. (1987) *Nature (London) 328*, 257–259.

Jeener, J., Meier, B. H., Bachmann, P., & Ernst, R. R. (1979) *J. Chem. Phys. 71*, 4546–4553.

Kaiser, E., Colescott, R. L., Bossinger, C. D., & Cook, P. I. (1970) *Anal. Biochem. 34*, 595–598.

Marion, D., & Wüthrich, K. (1983) *Biochem. Biophys. Res. Commun. 113*, 967–974.

Miller, L. H., Howard, R. J., Carter, R., Good, M. F., Nussenzweig, V., & Nussenzweig, R. S. (1986) *Science 234*, 1349–1356.

Nussenzweig, V., & Nussenzweig, R. S. (1985) *Cell 42*, 401–403.

Otting, G, Widmer, H., Wagner, G., & Wüthrich, K. (1986) *J. Magn. Reson. 66*, 187–193.

Patarroyo, M. E., Amador, R., Clavijo, P., Moreno, A., Guzman, F., Romero, P., Tascon, R., Franco, A., Murillo, L. A., Ponton, G., & Trujillo, G. (1988) *Nature (London) 332*, 158–161.

Piela, L., Nemēthy, G., & Scheraga, H. A. (1987) *Biopolymers 26*, 1587–1600.

Presta, L. G., & Rose, G. D. (1988) *Science 240*, 1632–1641.

Rance, M., Sorensen, O. W., Bodenhausen, G., Wagner, G., Ernst, R. R., & Wüthrich, K. (1983) *Biochem. Biophys. Res. Commun. 117*, 479–485.

Richardson, J. S., & Richardson, D. C. (1988) *Science 240*, 1648–1652.

Rose, G. D., Gierasch, L. M., & Smith, J. A. (1985) *Adv. Protein Chem. 37*, 1–106.

Satterthwait, A. C., Arrhenius, T., Hagopian, R. A., Zavala, F., Nussenzweig, V., & Lerner, R. A. (1989) *Philos. Trans. R. Soc. London, B 323*, 565–572.

Stewart, J. M., & Young, J. D. (1984) *Solid Phase Peptide Synthesis*, Pierce Chemical Co., Rockford, IL.

VanGeet, A. L. (1969) *Abstract of the 10th Experimental NMR Conferences*, March, 1969, Mellon Institute, Pittsburgh, PA.

Waltho, J. P., Feher, V. A., Lerner, R. A., & Wright, P. E. (1989) *FEBS Lett. 250*, 400–404.

Woody, R. W. (1974) in *Peptides, Polypeptides and Proteins* (Blout, E. R., Bovey, F. A., Goodman, M., & Lotan, N., Eds.) pp 338–348, Wiley, New York.

Wright, P. E., Dyson, H. J., & Lerner, R. A. (1988) *Biochemistry 27*, 7167–7175.

Wright, P. E., Dyson, H. J., Feher, V. A., Tennant, L. L., Waltho, J. P., Lerner, R. A., & Case, D. A. (1989) *UCLA Symp. Mol. Cell. Biol. New Ser. 109*, 1–13.

Wüthrich, K., Billeter, M., & Braun, W. (1984) *J. Mol. Biol. 180*, 715–740.

Zuiderweg, E. R. P., Boelens, R., & Kaptein, R. (1985) *Biopolymers 24*, 601–611.